



DA 362: A Gamma-Ray-emitting Compact Symmetric Object

Subhashree Swain¹, Vaidehi S. Paliya¹, D. J. Saikia¹, and C. S. Stalin²¹ Inter-University Centre for Astronomy and Astrophysics (IUCAA), SPPU Campus, Pune 411007, India; subhashree.swain@iucaa.in, vaidehi.s.paliya@gmail.com² Indian Institute of Astrophysics, Block II, Koramangala, Bengaluru 560034, Karnataka, India

Received 2024 October 21; revised 2024 December 13; accepted 2024 December 16; published 2025 January 21

Abstract

The γ -ray detection from an astrophysical object indicates the presence of an extreme environment where high-energy radiation is produced. With the continuous monitoring of the γ -ray sky by the Fermi Large Area Telescope (LAT) leading to deeper sensitivity, high-energy γ -ray emission has now been detected from a diverse class of jetted active galactic nuclei (AGNs). Here, we present the results of a multiwavelength study of the radio source DA 362, which was reported to be a blazar candidate of uncertain type. However, it was recently identified as a bona fide compact symmetric object (CSO) based on its subkiloparsec, bipolar radio morphology, and lack of radio variability. This makes DA 362 only the fourth γ -ray-emitting object of this enigmatic class of radio-loud AGNs. Using five very-long-baseline interferometry observations covering 1996–2018, we found the jet separation velocity to be subluminal ($v_{\text{app}} \sim 0.2c$), thus supporting its CSO nature. Its Fermi-LAT observations revealed a γ -ray flaring activity, a phenomenon never detected from the other three γ -ray-detected CSOs. This object is bright in the near-infrared band but extremely faint in the optical-UV filters, hinting at possible obscuration. Swift X-Ray Telescope observation of DA 362 reveals an extremely hard X-ray spectrum, though a strong claim cannot be made due to large uncertainties. We conclude that deeper observations are needed to probe the broadband properties of this enigmatic object and to understand the origin of high-energy γ -ray emission.

Unified Astronomy Thesaurus concepts: BL Lacertae objects (158); Radio jets (1347); Gamma-ray astronomy (628); Relativistic jets (1390)


1. Introduction

Compact symmetric objects (CSOs) are a special class of active galactic nuclei (AGNs) hosting subkiloparsec-scale jets and exhibiting symmetric radio morphologies (e.g., M. Orienti 2016). They are thought to host misaligned jets, and hence the observed broadband emission is not expected to be beamed (see P. N. Wilkinson et al. 1994; A. C. S. Readhead et al. 1996). These enigmatic objects are likely to be in the early stage of their evolution, with kinematic ages smaller than a few thousand years (e.g., A. C. S. Readhead et al. 1996). The small sizes of CSOs could be due to their young age, dense galactic environment inhibiting the jet propagation, and/or recurrent/transient episodes of nuclear jet activity (see C. P. O’Dea & D. J. Saikia 2021, for a review). From analysis of their relative numbers and redshift and linear size distributions, S. Kiehlmann et al. (2024b) present strong evidence that CSOs do not evolve into larger-scale radio sources and that they should be considered as a distinct “short-lived” jetted AGN population rather than “young” AGNs (see also A. C. S. Readhead et al. 2024).

The number of detected γ -ray-emitting CSOs has remained tiny compared to more common Fanaroff–Riley type I and II misaligned jetted AGNs and blazars. Only three CSOs have been reported via detections with the Fermi Large Area Telescope (LAT): TXS 0128+554 ($z=0.036$, associated with the γ -ray source 4FGL J0131.2+5547; M. L. Lister et al. 2020), NGC 3894 ($z=0.012$, counterpart of 4FGL J1149.0+5924; G. Principe et al. 2020), and NGC 6328 ($z=0.015$, associated with 4FGL J1724.2–6501; G. Migliori et al. 2016). All of them are located in the nearby Universe ($z < 0.05$), and their

proximity could be the primary reason for their Fermi-LAT detection if the γ -ray emission is unbeamed (e.g., G. Principe et al. 2021). The γ rays can be produced by hadronic mechanisms or due to the interaction of the relativistic electrons present in the lobes with the low-energy optical-UV photons originating from the accretion disk (see Ł. Stawarz et al. 2008; M. Kino & K. Asano 2011). Radio lobes typically expand with subrelativistic velocities; therefore, the γ -ray radiation is not expected to show significant flux variations, especially on short timescales (\sim weeks to months). Indeed, none of the three γ -ray-detected CSOs have exhibited significant flux variability as of now (S. Abdollahi et al. 2023). However, a definite conclusion cannot be drawn given the small number of known γ -ray-emitting CSOs. Increasing the sample size of these peculiar sources is also crucial to investigate the radiative processes powering their jets and their interaction with the surrounding environment, compare them with other non- γ -ray-detected CSOs, and understand their evolution.

Recently, S. Kiehlmann et al. (2024a) presented a comprehensive catalog of 79 CSOs obtained from the literature and by analyzing their multifrequency radio observations. They adopted the following four criteria: (i) a projected jet length < 1 kpc, (ii) detection of bipolar radio emission, (iii) nonvariable nature, and (iv) no superluminal motion detection in excess of $v_{\text{app}} = 2.5c$. In order to identify potential γ -ray-emitting CSOs, we cross-matched the CSO catalog with the fourth data release of the fourth γ -ray source catalog of Fermi-LAT-detected objects (4FGL-DR4; S. Abdollahi et al. 2020; J. Ballet et al. 2023). Using a search radius of $5''$, this exercise led to the identification of four γ -ray sources.³ Among them,

 Original content from this work may be used under the terms of the [Creative Commons Attribution 4.0 licence](https://creativecommons.org/licenses/by/4.0/). Any further distribution of this work must maintain attribution to the author(s) and the title of the work, journal citation and DOI.

³ In the sample of S. Kiehlmann et al. (2024a) there is a CSO, B3 0822+394, whose γ -ray detection was claimed by Y. Gu et al. (2022). However, this object is not reported as a γ -ray source in the 4FGL-DR4 catalog. Therefore, it did not appear in our final sample of γ -ray-emitting CSOs.

three have already been reported as γ -ray-emitting CSOs in earlier works (G. Migliori et al. 2016; M. L. Lister et al. 2020; G. Principe et al. 2020). The fourth object, DA 362 (B2 1413 +34), which is associated with the γ -ray source 4FGL J1416.0 +3443, is classified as a blazar candidate of uncertain type in the 4FGL-DR4 catalog. However, as shown by S. Kiehlmann et al. (2024a), this object is a bona fide CSO, thereby making it only the fourth γ -ray-detected object of this class. Moreover, L. Baldini et al. (2021) reported the detection of transient elevated γ -ray activity from this object. In this article, we present the results of an investigation of its multiwavelength properties utilizing >15 yr of Fermi-LAT data and other low-frequency observations and compare them with other γ -ray-detected CSOs. Section 2 elaborates on the data reduction steps. The results are presented in Section 3, and discussed in Section 4. We summarize our findings in Section 5. Throughout, we adopt the convention $S_\nu \sim \nu^\alpha$ for spectral index α , and use the cosmological parameters $\Omega_m = 0.27$, $\Omega_\Lambda = 0.73$, and $H_0 = 70 \text{ km s}^{-1} \text{ Mpc}^{-1}$.

2. Data Reduction and Analysis

2.1. Fermi-LAT

We followed the standard data reduction procedure to analyze the Fermi-LAT Pass 8 data of DA 362 covering 2008 August 4 to 2024 April 5 (MJD 54683–60405). We considered SOURCE class events in the energy range 0.1–300 GeV and lying within a region of interest of radius 15° centered at the target AGN. To avoid contamination from Earth's albedo, a zenith angle cut of $z_{\text{max}} < 90^\circ$ was also applied. All 4FGL-DR4 cataloged sources located within 20° of DA 362 position were considered to model the γ -ray sky in the likelihood fitting. To take into account the diffuse background emission, we adopted the Galactic and isotropic background templates provided by the Fermi Science Support Center.⁴ The γ -ray spectral parameters of all sources were first optimized, and then the final likelihood fitting was performed by varying the parameters of all sources with detection significance $>5\sigma$ (test statistic, $\text{TS} > 25$; J. R. Mattox et al. 1996).

We also generated the γ -ray spectrum (in six energy bins covering 0.1–300 GeV) and monthly binned light curve of DA 362 with the same settings described above. In the time/energy bins of nondetections ($\text{TS} < 9$), we computed flux upper limits at 95% confidence level.

2.2. Swift

The Neil Gehrels Swift satellite observed DA 362 on 2023 March 31 and 2023 April 5 (target ID: 15938, PI: Paliya). The Swift X-Ray Telescope (XRT) data were analyzed using the online Swift-XRT data products generator (P. A. Evans et al. 2009).⁵ Since there were no previous X-ray observations of the source, we first checked its X-ray detection. An X-ray source was found at the R.A. of $14^{\text{h}} 16^{\text{m}} 04^{\text{s}}.03$ and decl. of $+34^\circ 44' 34.8''$, with a 90% confidence radius of $5.7''$. The angular separation between the optimized X-ray and radio positions was estimated to be $2.5''$, thus confirming that the X-ray source is spatially consistent with DA 362. Given the low-exposure individual pointings, we added both observations to generate a combined X-ray spectrum with a net exposure of 4.2 ks in

which a net 22 counts were detected from the source. The obtained spectrum was grouped using the task `grppha` to have at least one count per bin, and the C-statistic was employed for the spectral fitting in XSPEC (K. A. Arnaud 1996). Uncertainties were estimated at 90% confidence level. For the purpose of plotting, the fitted X-ray spectrum was rebinned to have at least 3σ detection in each bin or grouped in sets of three bins.

The Swift UltraViolet and Optical Telescope (UVOT) data were reduced following the recommended guidelines. DA 362 was observed in two UV filters, namely UVM1 and UVM2. We combined the individual frames using the task `uvotimsum`. For the photometry, we applied the command `uvot-source`. The source was undetected, with UVM2 and UVM1 magnitudes fainter than 19.21 and 21.01 (Vega system), respectively.

2.3. Radio Observations

The five epochs of very-long-baseline interferometry (VLBI) observations of DA 362 covering 22 yr (1996–2018) are provided on the Astrogeno website (L. Petrov 2021).⁶ Four observations were in the *X* and *S* bands, and one epoch of data was taken in the *C* band. Additionally, the source was also detected in the Low-Frequency Array Two-meter Sky Survey, the Very Large Array Sky Survey, and the Rapid ASKAP Continuum Survey (M. Lacy et al. 2020; T. W. Shimwell et al. 2022; S. W. Duchesne et al. 2024).

2.4. Other Observations

We collected archival flux measurements from the Space Science Data Center.⁷ These data sets were published in several radio-to-optical/UV catalogs (G. Neugebauer et al. 1984; A. Wright & R. Otrupcek 1990; N. Epchtein et al. 1994; A. E. Wright et al. 1994; P. C. Gregory et al. 1996; J. J. Condon et al. 1998; T. Mauch et al. 2003; M. F. Skrutskie et al. 2006; S. E. Healey et al. 2007; E. L. Wright et al. 2010; I. Yamamura et al. 2010; V. N. Yershov 2014; D. J. Helfand et al. 2015; R. Ahumada et al. 2020). Since DA 362 was undetected in the Swift-UVOT data analysis, we checked whether it was included in the Panoramic Survey Telescope and Rapid Response System catalog (PanSTARRS; K. C. Chambers et al. 2016). A faint optical source positionally consistent with DA 362 was identified.

3. Results

Only three CSOs were identified in the γ -ray band prior to this work, making DA 362 the only fourth γ -ray-emitting object of this class. It is included in the 4FGL-DR4 catalog but was missing from previous Fermi-LAT catalogs. We carried out a dedicated data reduction covering the first ~ 15.75 yr of the Fermi-LAT operation. We also optimized the γ -ray source position of 4FGL J1416.0+3443 and estimated it to be R.A. = $14^{\text{h}} 15^{\text{m}} 55^{\text{s}}$ and decl. = $34^\circ 41' 18''$. The 95% uncertainty in the measured position is 0.07° . We show the TS map of the γ -ray region in Figure 1, where the radio and optimized γ -ray positions are also overlaid. Within the 95% uncertainty region, both positions are consistent, thus confirming the association of DA 362 with the γ -ray source 4FGL

⁴ <https://fermi.gsfc.nasa.gov/ssc/data/access/lat/BackgroundModels.html>

⁵ https://www.swift.ac.uk/user_objects/

⁶ <http://astrogeo.org>

⁷ <https://tools.ssdc.asi.it/SED/>

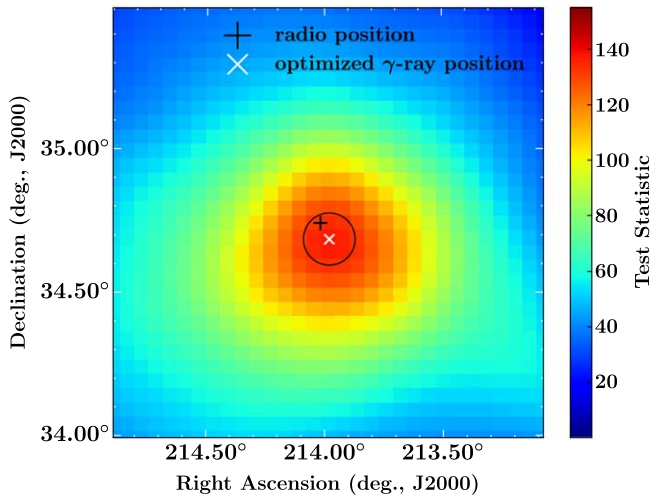


Figure 1. Test statistic map of the γ -ray sky centered at the optimized γ -ray position of DA 362. The black circle shows the 95% uncertainty region for the γ -ray position. The radio position of DA 362 is highlighted with the “+” mark.

J1416.0+3443. The spectral parameters obtained from the power-law fit are reported in Table 1. For comparison, we also provide the spectral parameters of the other three γ -ray-detected CSOs obtained following the same methodology outlined in Section 2.1. The computed γ -ray spectral parameters are on average consistent with those published in previous works (see G. Principe et al. 2021). The minor differences, if any, could be mainly due to the different time periods for the Fermi-LAT data reduction done in our and previous works.

Furthermore, the monthly binned γ -ray light curve of DA 362 is shown in Figure 2. Though sporadically detected, the source remained mostly in quiescence during the first ~ 12 yr of the Fermi-LAT’s operation, thus explaining its absence in 4FGL-DR3 and earlier γ -ray catalogs. Interestingly, a flaring activity was identified during MJD 59075–59287. The brightest γ -ray flux was found to be $(1.3 \pm 0.2) \times 10^{-7}$ ph s $^{-1}$ cm $^{-2}$, which is 10 times larger than its mission-averaged flux value. The detection significance of the flare peak was found to be $\sim 8\sigma$ (TS = 61).

We fitted the Swift-XRT spectrum of DA 362 with a power-law model modified for the Galactic absorption fixed to the neutral hydrogen column density of $N_{\text{H}} = 1.32 \times 10^{20}$ cm $^{-2}$ (P. M. W. Kalberla et al. 2005). In the energy range of 0.3–10 keV, the estimated photon index and energy flux are $0.79_{-0.46}^{+0.52}$ and $7.25_{-3.17}^{+5.38} \times 10^{-13}$ erg s $^{-1}$ cm $^{-2}$, respectively (Figure 3). Given the fact that CSOs are typically misaligned jetted AGNs, the observation of such a flat X-ray spectrum indicates a strong absorption of soft X-ray emission usually observed in Compton-thick sources (e.g., I. Georgantopoulos et al. 2007; S. Marchesi et al. 2018). Therefore, we attempted adding a redshifted absorption component (ZTBABS in XSPEC) during the fit; however, the parameters could not be constrained due to fitting failure. To get an idea about the intrinsic absorption, we froze the photon index to 1.8 and 2, i.e., to typical values estimated for AGNs, during the XSPEC fit. We obtained fitted N_{H} values of $1.05_{-0.63}^{+1.02} \times 10^{22}$ cm $^{-2}$ and $1.22_{-0.69}^{+1.09} \times 10^{22}$ cm $^{-2}$, respectively. These results provide supporting evidence about the possible obscured nature of DA 362. Deeper spectral observations will be needed to

characterize the possible X-ray-obscured nature of this γ -ray-detected CSO.

DA 362 is extremely faint in the optical-UV band. It remained undetected in the Swift-UVOT observations. The PanSTARRS catalog reports a faint optical source, with g - and r -band magnitudes of 21.59 ± 0.14 and 21.32 ± 0.18 , respectively, positionally consistent with the radio source. However, it remained undetected in the i and z filters. G. L. White (1992) reported its redshift to be $z = 0.26$, though its origin, whether spectroscopic or photometric, is unclear. The source lies in the Sloan Digital Sky Survey coverage area; however, it lacks spectroscopic measurement, likely due to its faintness. Moreover, C. Stanghellini et al. (1993) provided a limit of 24 and 23 mag in the r and i bands, respectively. In contrast, it is well detected in the mid-infrared (MIR) band covered by the Wide-field Infrared Survey Explorer (WISE).

The radio structure of DA 362 has been known to consist of a prominent jet toward the northeast, a weaker counterlobe on the western side, and a prominent central component (see D. Dallacasa et al. 2013, and references therein). We utilized the five epochs of VLBI images covering 1996–2018 available in Astrogro (L. Petrov 2021) to determine the jet velocity. In the S -band and C -band observations, we determined the separation velocity between the central component C and the jet component E, which are well-imaged in all the maps at these frequencies (Figure 4). In the higher-frequency X band, where the source has been observed in four epochs, the central component is resolved into a double, labeled C1 and C2 in Figure 4. It is unclear which of these two components may be hosting the nucleus of the galaxy. The apparent transverse velocity $\beta_{\text{app}} = \mu d_{\theta}(1+z)/c$, where μ is the observed proper motion, d_{θ} the angular size distance, z is the redshift, and c the speed of light. A least-squares fit to the data shows the β_{app} between C and E, and C1 and C2 to be 0.21 ± 0.30 and 0.24 ± 0.16 , respectively, consistent with a CSO and not a blazar. The separation between C and E is 102 pc, indicating a kinematic age of ~ 1600 yr, assuming this velocity to be a constant. Extended emission beyond component E is seen, for example, in the lower-frequency L -band image (D. Dallacasa et al. 1995), where they quote a total angular extent of 40 mas (161 pc), suggesting a kinematic age of ~ 2500 yr for their outermost component. For DA 362, S. Kiehlmann et al. (2024a) reported the upper limit to the projected linear size to be 693 pc, considering the second lowest contours. On the other hand, we have reported the angular separation of the eastern component from the core by measuring it from the peak-to-peak positions of the core and the eastern hotspot.

4. Discussion

The detection of small, parsec-scale, bipolar radio emission and a subluminal motion, as revealed by VLBI data sets, provide unambiguous confirmation that DA 362 is a bona fide CSO, thereby making it only the fourth γ -ray-detected object of this class. On comparing its γ -ray spectral properties with the other three γ -ray-detected CSOs, we found that DA 362 is the brightest among them and exhibits a spectrum steeper than the other sources. In the γ -ray luminosity versus photon index plane, DA 362 appears to lie in a region of high luminosity and soft spectrum (Figure 5, top-left panel). The γ -ray luminosity of the source was calculated assuming $z = 0.26$ (G. L. White 1992). Given that the origin of the redshift is uncertain, a γ -ray luminosity more than an order of magnitude larger than other

Table 1
Gamma- and X-Ray Spectral Parameters of DA 362 and Other Gamma-Ray-emitting CSOs as Derived from the Fermi-LAT and Swift-XRT Data Analyses, Respectively

4FGL Name	Counterpart	Gamma-Ray Results		TS
		$F_{0.1-300 \text{ GeV}}$ ($10^{-8} \text{ ph s}^{-1} \text{ cm}^{-2}$)	$\Gamma_{0.1-300 \text{ GeV}}$	
J1416.0+3443	DA 362	1.26 ± 0.07	2.71 ± 0.02	166
J0131.2+5547	TXS 0128+554	0.56 ± 0.02	2.05 ± 0.02	211
J1149.0+5924	NGC 3894	0.32 ± 0.09	2.16 ± 0.10	133
J1724.2-6501	NGC 6328	0.37 ± 0.12	2.28 ± 0.12	48

	Exposure (ks)	X-Ray Results		C-stat/dof
		$F_{0.3-10 \text{ keV}}$ ($10^{-13} \text{ erg s}^{-1} \text{ cm}^{-2}$)	$\Gamma_{0.3-10 \text{ keV}}$	
J1416.0+3443	4.2	7.25	$0.79^{+0.52}_{-0.46}$	22.17/22
J0131.2+5547	19.2	4.08	$3.11^{+0.37}_{-0.36}$	107.94/103
J1149.0+5924	5.5	$1.74^{+1.41}_{-1.74}$	$1.57^{+2.20}_{-3.20}$	12.71/11
J1724.2-6501	35.6	$7.44^{+1.34}_{-0.71}$	$1.66^{+0.23}_{-0.22}$	260.59/263

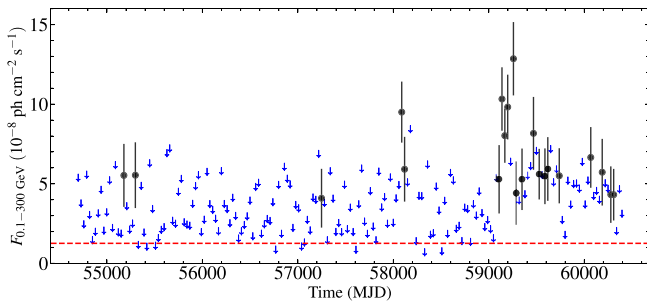


Figure 2. The monthly binned γ -ray light curve of DA 362. The 95% flux upper limits are shown with the downward arrows. The horizontal dashed line refers to the mission-averaged γ -ray flux of the source.

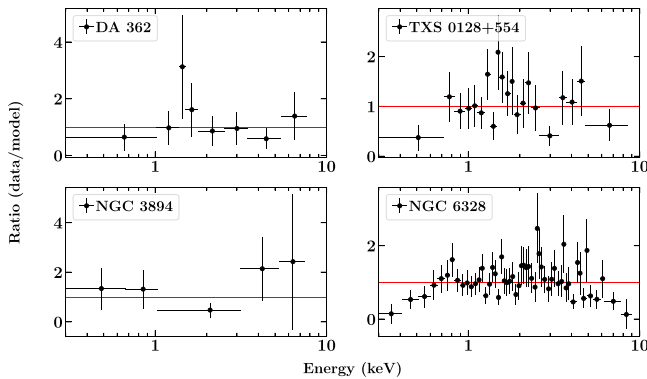


Figure 3. The residuals of the power-law model fitting with Galactic absorption.

CSOs should be treated with caution. We also compared the radio and γ -ray luminosities of CSOs with other jetted AGNs in the top-middle panel of Figure 5 adopting the 8 GHz VLBI flux densities reported in the Radio Fundamental Catalog. In this diagram, DA 362 appears to follow the observed correlation between the radio and γ -ray luminosities that have larger values compared to other γ -ray-detected CSOs.

The γ -ray emission detected from CSOs is not expected to exhibit significant variability if it originated from the radio lobes. Indeed, none of the three γ -ray-emitting CSOs have displayed any flux variability so far. However, a γ -ray flaring activity of DA 362 was identified with the Fermi-LAT

(Figure 2; see also L. Baldini et al. 2021). This observation suggests the γ -ray emission to be likely produced in the inner regions of the jet/core and not by the radio lobes. Similar results were found for another γ -ray-emitting CSO, TXS 0128+554 (M. L. Lister et al. 2020). However, given the low photon statistics, it is not possible to quantify the flux variability timescales to derive meaningful constraints on the location of the emission region.

We considered the Swift-XRT data of three other γ -ray-emitting CSOs for comparison, and adopted the same data reduction and spectral fitting methodology described in Section 2.2. In particular, TXS 0128+554 was serendipitously detected when Swift-XRT was observing GRB 190203a (target ID: 88751). The Swift-XRT was pointed to NGC 3894 once (target ID: 89108) and it was also serendipitously observed during the Swift Gravitational Wave Galaxy Survey (target IDs: 3107061, 3105839). On the other hand, NGC 6328 was observed 13 times (target IDs: 31815, 89109). We added individual observations to generate a combined X-ray spectrum for every CSO. The obtained net counts were 124, 12, and 413, for TXS 0128+554, NGC 3894, and NGC 6328, respectively.

We fitted a model including a power-law component and Galactic and intrinsic absorption. For TXS 128+554 and NGC 3894, the intrinsic neutral hydrogen column density could not be constrained, and hence was frozen to the values reported in recent works (M. L. Lister et al. 2020; K. Balasubramaniam et al. 2021). For NGC 6328, on the other hand, the data quality was good enough to determine the intrinsic column density. This was estimated to be $1.39^{+0.80}_{-0.70} \times 10^{21} \text{ cm}^{-2}$, which is consistent with that obtained by E. Bronzini et al. (2024). The obtained parameters are provided in Table 1 and we show the residuals of the fit in Figure 3. The unfolded spectra, in νF_ν versus ν format, were extracted by rebinning them to have at least 5σ detection in each bin or grouped in sets of five bins. The Swift-XRT spectral fitting results for NGC 6328 were published by H. Matake & Y. Fukazawa (2023) and the spectral parameters estimated in this work are fully consistent with their published values. The Swift-XRT data fitting results are reported in this work for the first time for the three other sources. We note that NGC 3894 and NGC 6328 have also been observed with XMM-Newton, Chandra, and/or NuSTAR, and more complex spectral modeling has been performed on them (e.g.,

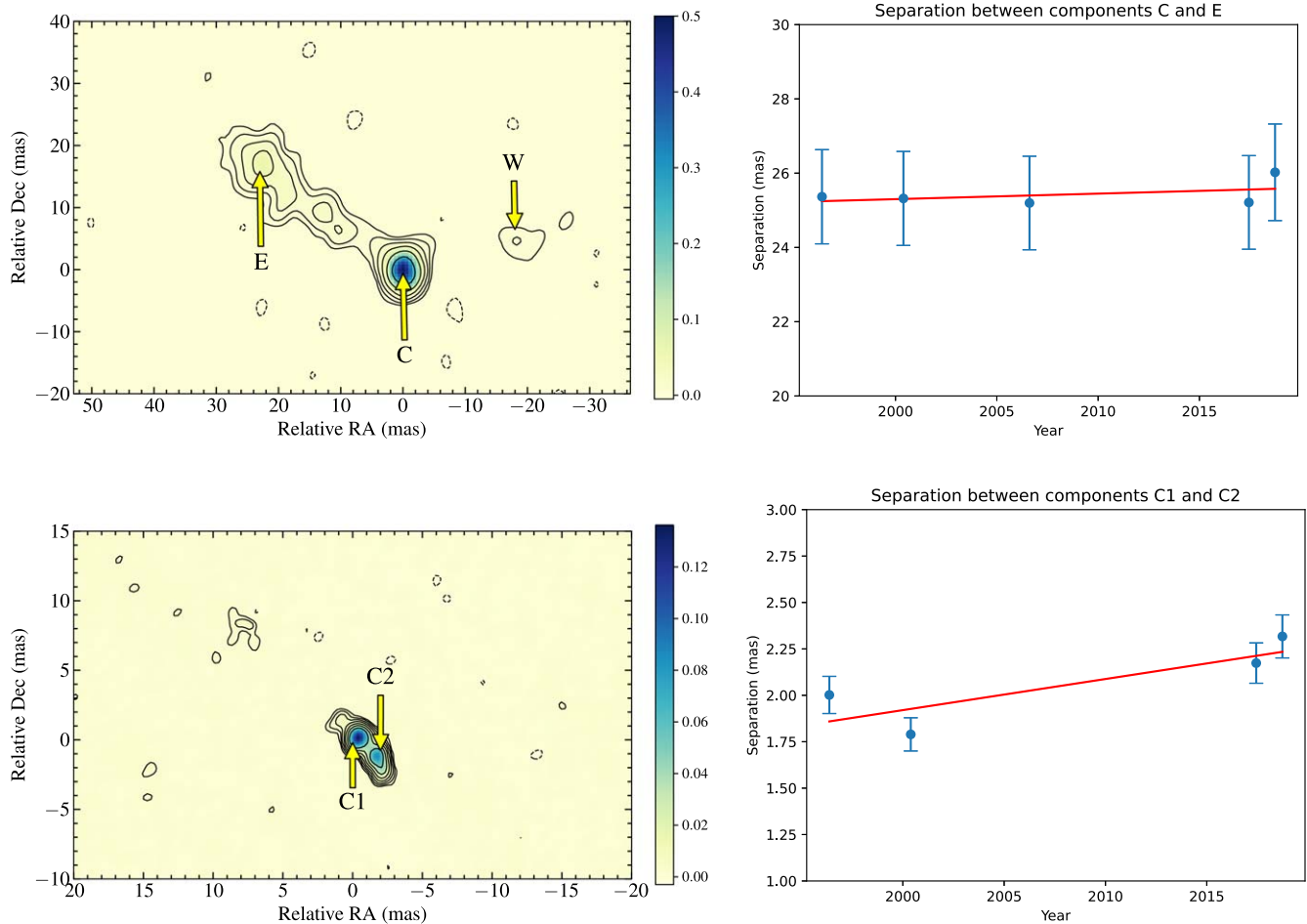


Figure 4. VLBA images of DA 362 at the S band (2.29 GHz, upper left) and X band (8.65 GHz, lower left) from observations on 2000 May 22 (from astrogeo.org, uploaded by Alexandr Pushkarev). The contour levels are $3\sigma \times -1, 1, 2, 4, \dots$, where σ is 1.1 and 0.7 mJy beam $^{-1}$ for the S- and X-band images, respectively. The linear least-squares fit to the separations between components C and E (upper right) and C1 and C2 (lower right) are shown for the available data from astrogeo.org.

K. Balasubramaniam et al. 2021; M. Sobolewska et al. 2022; E. Bronzini et al. 2024). High-quality X-ray observations of DA 362, e.g., with XMM-Newton, will be needed to test physically motivated spectral models as done for other γ -ray-detected CSOs.

On comparing the Swift-XRT spectral parameters of DA 362 with those estimated for other γ -ray-detected CSOs, we found that it has an absorption-corrected 0.3–10 keV flux brightness, similar to other sources, though the uncertainties in the flux value are large, possibly due to low exposure. While other γ -ray-emitting CSOs have X-ray photon indices similar to that typically observed from γ -ray-emitting radio galaxies (see H. Matake & Y. Fukazawa 2023), DA 362 exhibits an extremely hard X-ray spectrum. Usually, such a flat X-ray spectrum is observed from Compton-thick AGNs due to severe absorption of the soft X-ray photons. Interestingly, the WISE observations indicate it to be bright in the MIR band, while the source is extremely faint in the optical-UV band, thus making it a very red object. Combining the MIR-to-UV photometric results with the X-ray spectral parameters, a picture emerges hinting at strong dust obscuration, supporting the possible obscured nature of DA 362. Deeper X-ray observations will be crucial to test this scenario.

In the WISE color-color diagram of γ -ray sources, DA 362 appears to lie in a region mainly populated by flat-spectrum radio quasars (Figure 5, top-right panel). Therefore, its MIR

emission could originate via synchrotron emission produced by compact radio lobes expanding with mildly relativistic velocities that may not be beamed. In contrast, other γ -ray-emitting CSOs are located in an area dominated by elliptical galaxies. A possible explanation could be that the MIR emission observed from these objects is primarily dominated by the thermal radiation from the host galaxy (see also E. Kosmaczewski et al. 2020). DA 362, on the other hand, lies in a region mainly occupied by quasars/Seyferts (S. Mateos et al. 2012; D. Stern et al. 2012), which also includes the three sources marked as Compton thick in E. Kosmaczewski et al. (2020), as well as a few other CSOs.

The broadband spectral energy distribution (SED) of DA 362 is shown in the bottom-left panel of Figure 5. For comparison, we also plot the SEDs of the other three γ -ray-emitting CSOs that have also been studied in previous works (M. L. Lister et al. 2020; K. Balasubramaniam et al. 2021; M. Sobolewska et al. 2022; E. Bronzini et al. 2024). At GHz frequencies, DA 362 has a brightness similar to TXS 0128 +554 and NGC 3894, though fainter than NGC 6328. The primary difference can be seen in the MIR-to-UV energy range, where the observed emission is dominated by the host galaxy for other γ -ray-emitting CSOs, which is not the case for DA 362. Deep optical-MIR photometric and spectroscopic observations are needed to characterize its host galaxy properties and accretion activity. We discussed the comparison of the X- and

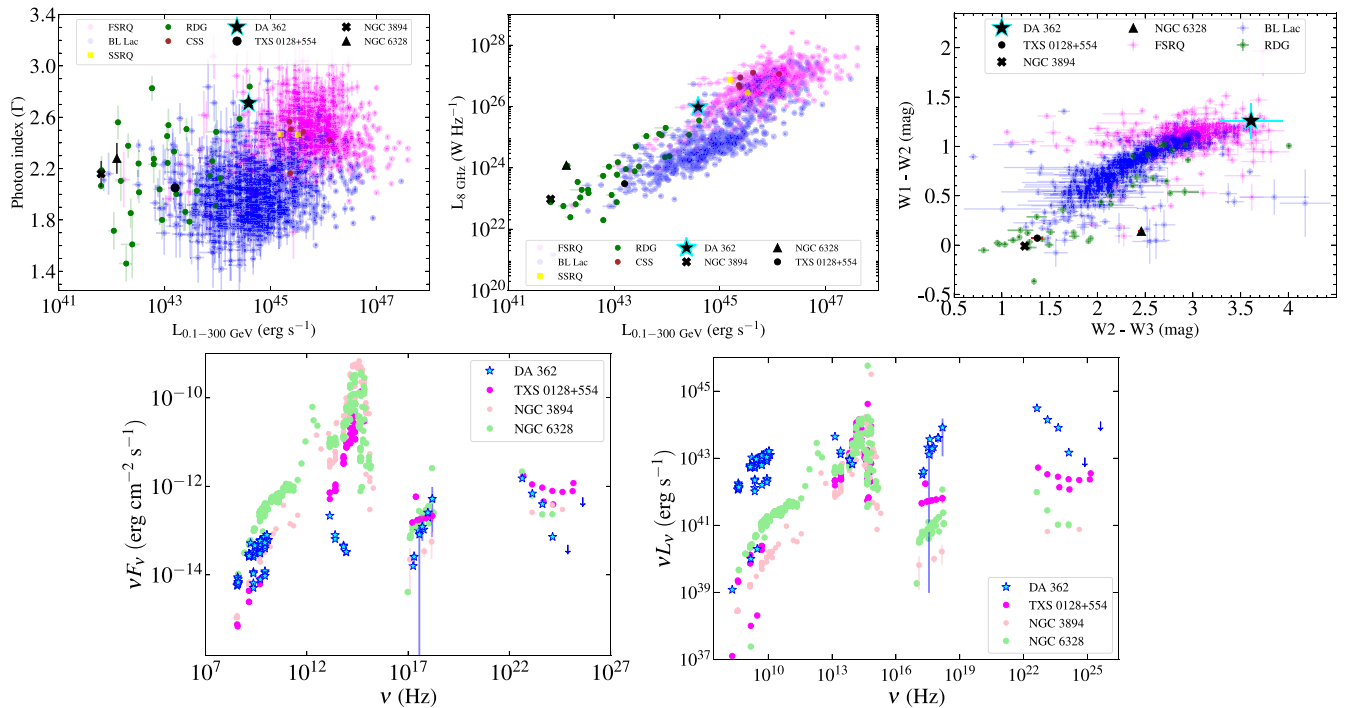


Figure 5. Plots of the γ -ray luminosity vs. spectral index and those of radio vs. γ -ray luminosities are shown in the top-left and top-middle panels. The top-right panel shows the WISE color-color diagram. Blue and pink circles denote BL Lac objects and flat-spectrum radio quasars, respectively. The yellow rectangle, green circles, and brown circles refer to steep spectrum radio quasars, radio galaxies, and compact steep spectrum sources, respectively. These γ -ray sources were selected from the 4FGL-DR4 catalog (S. Abdollahi et al. 2020; J. Ballet et al. 2023). We also show γ -ray-detected CSOs, as labeled. Broadband spectral energy distributions of the γ -ray-detected CSOs are plotted in the bottom panels.

γ -ray properties earlier in this section, and the observed SEDs at these energies are consistent with the reported findings. We also show the multiwavelength SEDs of γ -ray-emitting CSOs in the νL_ν versus ν plane in the bottom-right panel of Figure 5. Given the larger redshift of DA 362, it appears more luminous compared to other γ -ray-detected CSOs at all wavelengths, except at optical frequencies, where it is less luminous. However, since the redshift information of DA 362 is tentative, firm conclusions about its nature cannot be drawn.

5. Summary

In this work, we have studied the multiwavelength properties of a CSO, DA 362, which was recently found to be a γ -ray emitter by Fermi-LAT, thereby making it only the fourth γ -ray-detected object of this class of AGNs. We summarize our key findings below:

1. We confirm the association of the γ -ray source 4FGL J1416.0+3443 with DA 362 by analyzing ~ 15.75 yr of Fermi-LAT data. The optimized γ -ray position was consistent with the radio source within the estimated 95% γ -ray uncertainty region.
2. The monthly binned γ -ray light curve of DA 362 revealed a flaring activity during MJD 59075–59287. This is the first detection of a γ -ray flare from a CSO, which was also reported by L. Baldini et al. (2021). This peculiar flaring activity indicates that the γ -ray emission originates from the core/jet rather than from the radio lobes.
3. The source exhibits an extremely hard X-ray spectrum ($0.3\text{--}10 \text{ keV}$, photon index = $0.79_{-0.46}^{+0.52}$) as found with the analysis of the low-exposure Swift-XRT data. However, a strong claim cannot be made due to large uncertainties.

4. DA 362 is bright in the MIR but extremely faint in the optical band, thus suggesting possible dust obscuration. By also considering the observed X-ray spectral shape, these results indicate the possible X-ray-obscured nature of the source.
5. We used calibrated VLBI images from the Astrogoo website, and estimated the jet separation velocity to be $v_{\text{app}} \sim 0.2c$. This detection of a subluminal motion further supports the CSO nature of DA 362.
6. The available observations have provided tantalizing clues about the enigmatic behavior of this γ -ray-emitting CSO. Deeper observations with sensitive observing facilities will be needed to explore the broadband physical properties of DA 362 and probe the origin of γ -ray emission.





Acknowledgments

We thank the journal referee for constructive criticism. Thanks to the Swift satellite's principal investigator, Brad Cenko, for approving the observation request. Part of this work is based on archival data, software, or online services provided by the Space Science Data Center – ASI. This research has made use of NASA's Astrophysics Data System Bibliographic Services. This research has made use of data obtained through the High Energy Astrophysics Science Archive Research Center Online Service, provided by the NASA/Goddard Space Flight Center.

Facilities: Swift, Fermi.

Software: XSPEC (v12.10.1; K. A. Arnaud 1996), Swift-XRT data product generator (P. A. Evans et al. 2009), fermiPy (M. Wood et al. 2017).

ORCID iDs

Subhashree Swain  <https://orcid.org/0009-0006-2098-2592>
 Vaidehi S. Paliya  <https://orcid.org/0000-0001-7774-5308>
 D. J. Saikia  <https://orcid.org/0000-0002-4464-8023>
 C. S. Stalin  <https://orcid.org/0000-0002-4998-1861>

References

- Abdollahi, S., Acero, F., Ackermann, M., et al. 2020, *ApJS*, 247, 33
 Abdollahi, S., Ajello, M., Baldini, L., et al. 2023, *ApJS*, 265, 31
 Ahumada, R., Allende Prieto, C., Almeida, A., et al. 2020, *ApJS*, 249, 3
 Arnaud, K. A. 1996, in ASP Conf. Ser. 101, *Astronomical Data Analysis Software and Systems V*, ed. G. H. Jacoby & J. Barnes (San Francisco, CA: ASP), 17
 Balasubramaniam, K., Stawarz, Ł., Cheung, C. C., et al. 2021, *ApJ*, 922, 84
 Baldini, L., Ballet, J., Bastieri, D., et al. 2021, *ApJS*, 256, 13
 Ballet, J., Bruel, P., Burnett, T. H., Lott, B. & The Fermi-LAT collaboration 2023, arXiv:2307.12546
 Bronzini, E., Migliori, G., Vignali, C., et al. 2024, *A&A*, 684, A65
 Chambers, K. C., Magnier, E. A., Metcalfe, N., et al. 2016, arXiv:1612.05560
 Condon, J. J., Cotton, W. D., Greisen, E. W., et al. 1998, *AJ*, 115, 1693
 Dallacasa, D., Fanti, C., Fanti, R., Schilizzi, R. T., & Spencer, R. E. 1995, *A&A*, 295, 27
 Dallacasa, D., Orienti, M., Fanti, C., Fanti, R., & Stanghellini, C. 2013, *MNRAS*, 433, 147
 Duchesne, S. W., Grundy, J. A., Heald, G. H., et al. 2024, *PASA*, 41, e003
 Epchtein, N., de Batz, B., Copet, E., et al. 1994, *Ap&SS*, 217, 3
 Evans, P. A., Beardmore, A. P., Page, K. L., et al. 2009, *MNRAS*, 397, 1177
 Georgantopoulos, I., Georgakakis, A., & Akylas, A. 2007, *A&A*, 466, 823
 Gregory, P. C., Scott, W. K., Douglas, K., & Condon, J. J. 1996, *ApJS*, 103, 427
 Gu, Y., Zhang, H.-M., Gan, Y.-Y., et al. 2022, *ApJ*, 927, 221
 Healey, S. E., Romani, R. W., Taylor, G. B., et al. 2007, *ApJS*, 171, 61
 Helfand, D. J., White, R. L., & Becker, R. H. 2015, *ApJ*, 801, 26
 Kalberla, P. M. W., Burton, W. B., Hartmann, D., et al. 2005, *A&A*, 440, 775
 Kiehlmann, S., Lister, M. L., Readhead, A. C. S., et al. 2024a, *ApJ*, 961, 240
 Kiehlmann, S., Readhead, A. C. S., O'Neill, S., et al. 2024b, *ApJ*, 961, 241
 Kino, M., & Asano, K. 2011, *MNRAS*, 412, L20
 Kosmaczewski, E., Stawarz, Ł., Siemiginowska, A., et al. 2020, *ApJ*, 897, 164
 Lacy, M., Baum, S. A., Chandler, C. J., et al. 2020, *PASP*, 132, 035001
 Lister, M. L., Homan, D. C., Kovalev, Y. Y., et al. 2020, *ApJ*, 899, 141
 Marchesi, S., Ajello, M., Marcotulli, L., et al. 2018, *ApJ*, 854, 49
 Matake, H., & Fukazawa, Y. 2023, *PASJ*, 75, 1124
 Mateos, S., Alonso-Herrero, A., Carrera, F. J., et al. 2012, *MNRAS*, 426, 3271
 Mattox, J. R., Bertsch, D. L., Chiang, J., et al. 1996, *ApJ*, 461, 396
 Mauch, T., Murphy, T., Buttery, H. J., et al. 2003, *MNRAS*, 342, 1117
 Migliori, G., Siemiginowska, A., Sobolewska, M., et al. 2016, *ApJL*, 821, L31
 Neugebauer, G., Habing, H. J., van Duinen, R., et al. 1984, *ApJL*, 278, L1
 O'Dea, C. P., & Saikia, D. J. 2021, *A&ARv*, 29, 3
 Orienti, M. 2016, *AN*, 337, 9
 Petrov, L. 2021, *AJ*, 161, 14
 Principe, G., Di Venere, L., Orienti, M., et al. 2021, *MNRAS*, 507, 4564
 Principe, G., Migliori, G., Johnson, T. J., et al. 2020, *A&A*, 635, A185
 Readhead, A. C. S., Ravi, V., Blandford, R. D., et al. 2024, *ApJ*, 961, 242
 Readhead, A. C. S., Taylor, G. B., Xu, W., et al. 1996, *ApJ*, 460, 612
 Shimwell, T. W., Hardcastle, M. J., Tasse, C., et al. 2022, *A&A*, 659, A1
 Skrutskie, M. F., Cutri, R. M., Stiening, R., et al. 2006, *AJ*, 131, 1163
 Sobolewska, M., Migliori, G., Ostorero, L., et al. 2022, *ApJ*, 941, 52
 Stanghellini, C., O'Dea, C. P., Baum, S. A., & Laurikainen, E. 1993, *ApJS*, 88, 1
 Stawarz, Ł., Ostorero, L., Begelman, M. C., et al. 2008, *ApJ*, 680, 911
 Stern, D., Assef, R. J., Benford, D. J., et al. 2012, *ApJ*, 753, 30
 White, G. L. 1992, *PASA*, 10, 140
 Wilkinson, P. N., Polatidis, A. G., Readhead, A. C. S., Xu, W., & Pearson, T. J. 1994, *ApJL*, 432, L87
 Wood, M., Caputo, R., Charles, E., et al. 2017, *ICRC (Busan)*, 35, 824
 Wright, A., & Otrupcek, R. 1990, PKS Catalog, <https://cdsarc.cds.unistra.fr/viz-bin/cat/VIII/15>
 Wright, A. E., Griffith, M. R., Burke, B. F., & Ekers, R. D. 1994, *ApJS*, 91, 111
 Wright, E. L., Eisenhardt, P. R. M., Mainzer, A. K., et al. 2010, *AJ*, 140, 1868
 Yamamura, I., Makiuti, S., Ikeda, N., et al. 2010, *yCat*, 2298, 0
 Yershov, V. N. 2014, *Ap&SS*, 354, 97